ACS APPLIED MATERIALS & INTERFACES

RESEARCH ARTICLE

www.acsami.org

Fabrication of Monolayer of Polymer/Nanospheres Hybrid at a Water-Air Interface

Chi-Chih Ho,[†] Po-Yuan Chen,[†] Keng-Hui Lin,[†,‡] Wen-Tau Juan,[*,†] and Wei-Li Lee[*,†]

[†]Institute of Physics and [‡]Research Center of Applied Science, Academia Sinica, Nankang, Taipei, Taiwan R.O.C.

ABSTRACT: A new type of polymer-assisted self-assembly of nanospheres at a water−air interface was uncovered. By adding merely 1−3 ppm of polyethylene oxide in the water, the polystyrene nanospheres, applicable to diameters ranging from 100 nm to 1 μm, were found to gradually move closer to each other and eventually form a close-packed structure confirmed from its diffraction pattern. As it turns out, polyethylene oxides are adsorbed onto the surface of polystyrene nanospheres, giving rise to the effective screening of coulomb repulsive force between nanospheres followed by the onset of polymer-bridging effect as demonstrated from the strong suppression of Brownian motion. The resulting monolayer of close-packed polymer/nanospheres hybrid at the water−air interface with area size more than 1 cm^2 are robust and can be transferred to a substrate of any kind without serious breaking due to surface tension tearing. Our finding may provide a further extension to the scope of nanosphere lithography technique.

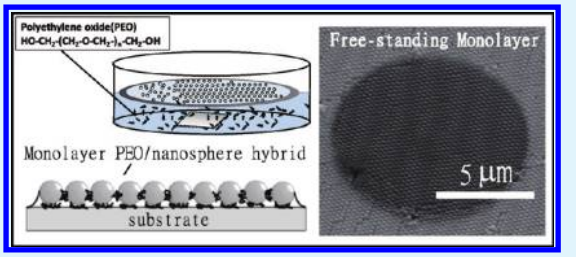

KEYWORDS: colloids, polymer materials, self-assembly, hybrid and composite materials, nanosphere lithography, water−air interface

INTRODUCTION

Nanosphere lithography (NSL) pioneered by Hulteen and van Duyne[1] in 1995 offers an approach at lower cost and better time efficiency to fabricate large area nanostructure systems that are difficult using conventional nano-fabrication technique. The function of NSL relies on a monolayer of monodisperse nanospheres (NSs) on a substrate as a template for structure patterning. Naturally, the biggest hurdle resides on the preparation of large area monolayer of close-packed NSs on a substrate, which turns out to be a challenging colloidal self-assembly problem, such that the highest number density can be achieved.

There are several methods that have been developed to tackle the problem. One is to utilize the depletion force[2,3] by adding a second species of NSs with smaller size to induce an entropically driven self-assembly of bigger NSs. Nevertheless, a substantial amount of smaller NSs are needed in order to observe the effect. Another method uses the surface tension to assemble the NSs, such as spin coating[4] and vertical pulling.[5−7] However, they are extremely sensitive to the interfacial properties that are substrate dependent. The resulting NSs packing domains are usually on the order of a few square micrometers and are susceptible to large cracks and vacancies because of the instability during the solvent evaporation.

On the other hand, the well-known Langmuir−Blodgett (LB) method[8−12] assembles the NSs, confined in an area at the water−air interface, via increasing the NS area fraction either by adding more NSs or by reducing the confining area. It has also been found that the addition of surfactant can effectively drive the NSs to assemble into close-packed structure.[8,13] The disadvantages in the LB method, however, are the strong repulsive force between NSs coming from the induced charges and the lack of strong binding between NSs. Even with surfactant, the NS packing structure is hard to maintain while transferring to a substrate that is not sufficiently flat. In addition, the surfactant greatly reduces the surface tension at water−air interface. Special care on adding surfactant is needed to avoid the submersion of monolayer NSs.

In light of those difficulties, we have developed an approach to prepare a monolayer of close-packed NSs that can be transferred to a substrate of any kind with area size larger than 1 cm^2. Using a modified LB method with the addition of merely a few parts per million water-soluble polyethylene oxide (PEO, a long chain polymer with formula $(OCH_2CH_2)_n$) in water, we uncovered a new type of self-assembly of NSs resulting from two main effects. One is the adsorption of PEOs onto polystyrene (PS) NSs that effectively screens the coulomb repulsive force between NSs. This in turn brings the NSs closer to each other. When NSs are close enough, the onset of polymer-bridging effect provides an additional bonding between NSs, making the monolayer NSs robust. The resulting monolayer PEO/NS hybrid can then be transferred to a substrate of any kind while still keeping its

Received: August 31, 2010
Accepted: December 8, 2010
Published: January 10, 2011

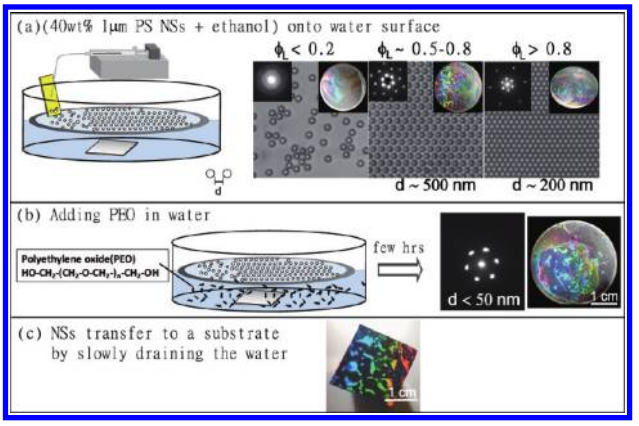

Figure 1. Procedure of preparing monolayer of close-packed PEO/NSs hybrid on a substrate. (a) 40 wt % monodisperse 1 μm PS NSs are mixed with ethanol and then carefully spread onto a water surface via a conduit plate (yellow). The diffraction pattern shows a hexagonal symmetry and enlargement in reciprocal lattice spacing as the NSs area fraction ϕ_L increases. (b) Abrupt changes in diffraction pattern and iridescent image a few hours after introducing PEOs into water. (c) Monolayer PEO/NSs hybrid transferred to a substrate by slowly draining the water. See text for detailed description.

original packing structure regardless of the substrate flatness and the surface tension tearing during the process.

EXPERIMENTAL SECTION

Materials. Monodisperse PS NS suspension in DI water was sulfonated and purchased from Duke Scientific with coefficient of variation (CV) less than 3% and diameters ranging from 100 nm to 1 μm. PEOs were obtained from Varian Inc. with molecular weight (MW) = 1 435 000 g/mol and MW/Mn < 1.3. Poly(styrenesulfonate sodium) (NaPSS) was Purchased from Sigma-Aldrich with averaged MW = 70 000 g/mol. These polymers and NS suspensions were used as received.

Assembly of Monolayer PEO/PS NSs Hybrid at Water−Air Interface. Figure 1 illustrates the experimental set-up for the preparation of close-packed monolayer of PEO/NSs hybrid at water−air interface. A clean Petri dish filled with high quality deionized (DI) water was first ultrasonicated for 10 min to remove excess gases trapped in the DI water followed by the extraction of scum and bubble that may form at the water−air interface. A thin Teflon ring with a diameter of 5 cm was then carefully placed at the water−air interface, serving as an area confinement for the NSs. The PS NSs suspension was first concentrated using a centrifuge to a value of C_n depending on the size of NSs. It was then mixed with ethanol at a volume ratio of γ and slowly injected at a rate of ~0.1−0.5 μL/min using a syringe pump onto the surface of a nearly vertical conduit plate (Figure 1a) before spreading over the water−air interface. This can minimize the harsh compression and irreversible NS aggregation due to the van der Waals forces.

For the best uniformity in NS distribution at the water−air interface, we used [C_n = 40 wt %, γ= 1:1] and [C_n = 10 wt %, γ = 2:1] for 1 μm and 220 nm NSs, respectively. (All nanosphere sizes mentioned here are in diameter.) The conduit plate comprises a silicon wafer with a thin layer of thermal oxide. It was first treated in oxygen plasma to further enhance its affinity for DI water and then soaked in a mixture of water and ethanol at equal volume for a period of time before use. When the NSs area fraction ϕ_L, defined as the ratio of area occupied by NSs to the Teflon ring area, was larger than 0.8, 1−3 ppm PEO was added in the DI water as shown in Figure 1b. After a few hours, a monolayer of PEO/NSs hybrid formed at the water−air interface.

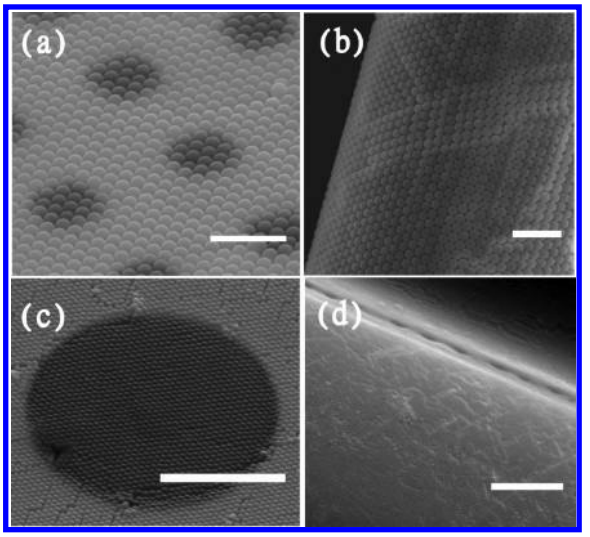

Figure 2. (a, c) SEM images of free-standing monolayers of 1 μm and 220 nm NSs/PEO hybrid, respectively. The darker areas are free-standing monolayers. (b, d) Transfer of monolayers of 1 μm and 220 nm NSs/PEO hybrid, respectively, onto the curved surface of a fine gold wire. The white scale bars are 5 μm.

Structure and Motion Characterization. A laser beam with λ = 532 nm and spot size of 3 mm in diameter was normally incident on the monolayer of NSs at water−air interface in order to obtain the corresponding diffraction pattern for the packing structure. Zeta potential measurement on PS NSs suspension was performed using a Malvern Zetasizer Nano ZS system. Brownian motion of NS was monitored by a Leica DM/LM/P microscope equipped with 100×/NA0.75 air objective and a high-speed Phantom V7.3M (sr: vr1008 8397) camera. The NS trajectories were then analyzed using Image J software and IDL program with the particle codes developed by J. Crocker and D. Crocker.

RESULTS AND DISCUSSION

Packing Structure at Water−Air Interface. At low NS area fraction $\phi_L \leq 0.2$, the distribution at the water−air interface is random. As ϕ_L increases to a value of ~0.5−0.8, it starts to develop a hexagonal symmetry in the diffraction pattern and an iridescent appearance as shown in the inset of Figure 1a. The separation d between NSs was estimated to be about 500 nm determined from the first-order and second-order peaks in the diffraction pattern. We found that d gradually drops to a value of 200 nm for ϕ_L above 0.8. No further decrease in d was found with further increase in ϕ_L, suggesting the presence of a strong repulsive force between them. Remarkably, after adding a small amount of PEOs into the DI water with resulting PEO concentration about 1−3 ppm (PEO radius of gyration $R_g \approx 30$ nm), we found a further enlargement of the reciprocal lattice spacing in the diffraction pattern. Eventually, only the first-order diffraction peaks appear, which casts an upper limit of $d \cong 50$ nm according to Ewald construction.[7,13,15] On the other hand, a clear reduction of the NSs area to about 60% of its original area size is apparent from the iridescent image shown in Figure 1b. Both results indicate an intriguing phenomenon of polymer-assisted self-assembly of NSs, which is the main focus of this report.

Transfer of Monolayer PEO/PS NSs Hybrid on a Substrate. The monolayer NSs can be transferred onto a substrate by slowly draining the water while still keeping its original packing structure as illustrated in Figure 1c. It can work well on substrates with

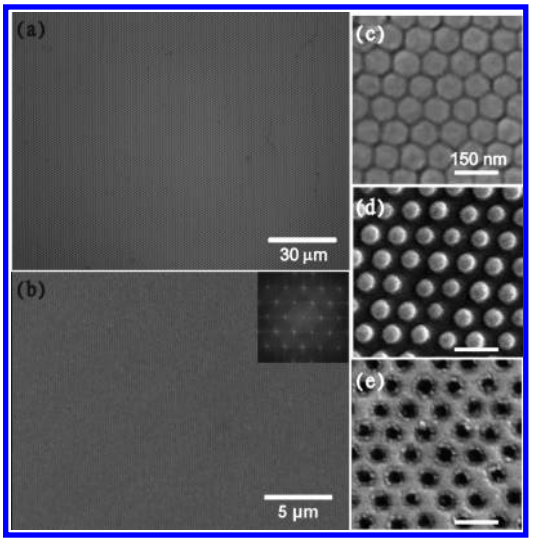

Figure 3. (a, b) SEM images of monolayer close-packed PEO/NSs hybrid with diameter 1 μm and 220 nm, respectively, on a Si(100) substrate. The inset of b is its corresponding FFT. The diameter (100 nm) of NSs shown in (c) can be reduced using oxygen plasma etching as demonstrated in (d) followed by thin film deposition and NSs removal. (e) Resulting nano-antidot thin films.

different surface condition and water affinity. We also carried out the transfer of PEO-bridged monolayer of NSs onto a fine gold wire and a silicon nitride substrate with hole array. The formation of free-standing membranes shown as darker regimes in images a and c in Figure 2 for monolayers of 1 μm and 220 nm NSs, respectively, provide a strong evidence for the bonding between NSs by PEO-bridging effect. On the other hand, the close-packed structure of NSs is well-preserved on the curved surface of a fine gold wire with a diameter of ~25 μm as demonstrated in images b and d in Figure 2 for monolayers of 1 μm and 220 nm NSs, respectively. This is of particular importance because of the difficulty in the nanostructure patterning on a curved surface using conventional tools.

Several different PEO concentrations up to 2000 ppm were used for the formation of PEO/NSs hybrid at water-air interface. When transferred onto a substrate with hole array of 3 μm in diameter as shown in Figure 2a, the ratio of the number of nonbreaking free-standing monolayer hybrid to the total number of holes covered by the monolayer hybrid was found to be more than 80% when the PEO concentration was higher than 500 ppm. This suggests that the bonding strength can be greatly improved by introducing more PEOs right before the transfer process. In addition, we also have used PEO with different MWs of 723 500 and 116 300 g/mol. The results were well-reproduced and consistent with that using MW = 1 435 000 g/mol.

Images a and b in Figure 3 show the SEM images of monolayer of close-packed PEO/NSs hybrid with diameter 1 μm and 220 nm, respectively, on Si(100) substrate prepared by this method. The nearly defect free regime is bigger than 100 μm × 100 μm and 30 μm × 30 μm for 1 μm and 220 nm NSs, respectively. The corresponding fast Fourier transform (FFT) shown in the inset of Figure 3b indicates a triangular lattice as expected. The PEOs are nearly invisible in the figure and hence have insignificant influence on the shape and size of NSs. However, for 100 nm NSs shown in Figure 3c, the distortion caused by PEOs seems to be more pronounced. This, in principle, can be minimized by using PEOs with smaller MW. Combining the results from diffraction patterns and also iridescent images, we found that the entire monolayer NS contains multiple domains with biggest packing domain size nominally larger than 3 mm × 3 mm. The domain boundary typically comprises twinning defects[16] and wrong-sized NSs because of the finite CV in the NS suspension we used. However, we remark that there is no major cracks and vacancies over the entire area such that the highest NSs number density is obtained over an area larger than 1 cm^2. The biggest domain size varies from sample to sample because of the poor control on the initial condition of NSs distribution at water-air interface using current approach. Further development of technique to evenly spread NSs on water−air interface is needed in order to extend the packing domain size. The resulting monolayer close-packed PEO/NSs hybrid on a substrate can then be used in NSL technique[1] to prepare large area nanostructure thin films as demonstrated in Figure 3c−e for 100 nm NS. Because of the close-packed structure over large area and the capability of tuning NSs diameters simply by oxygen plasma etching, physical properties in nanostructure thin films can then be quantitatively investigated using standard apparatus.[17]

Suppressed Brownian Motion and Polymer-Bridging Effect. The competition of attractive and repulsive forces between NSs floating at water-air interface is nontrivial. NSs normally contain surface charges arising from chemical functionality during the synthesis process. The resulting charged NSs at the water−air interface induce charge dipoles, giving rise to the dipole−dipole coulomb repulsive force.[22] On the other hand, the distorted water−air interface due to the presence of NSs either by gravity or by electric field can give rise to attractive capillary forces between NSs.[18−21] It was also pointed out that the inhomogeneous surface charge distribution on NSs produces a dipole component parallel to the interface plane, giving rise to an attractive force at shorter interparticle distances.[23] However, the balance between attractive and repulsive forces makes it advantageous to form two-dimensional colloidal crystal with a finite d between NSs, which agrees well with our observation shown in Figure 1a.

When introducing PEOs into water, depletion interaction needs to be taken into account. It, basically originates from the addition of polymers smaller in size, resulting in an additional attractive force between NSs such that more volume accessible to the polymers can be released. The free energy gain equals $(D\pi R_g^2 n_p)k_BT$,[2,3] where D and n_p are the diameter of NSs and the number density of the polymer, respectively. Using our experimental parameters, the free energy gain was estimated to be on the order of $1 \times 10^{-3}\ k_BT$, which is too small to account for the observed PEO-assisted self-assembly of NSs at the water−air interface. Furthermore, there is no significant variation in the surface tension throughout the range of PEO concentration we have used.

On the other hand, inspired from the observation of PEO residues on NSs from SEM image shown in the inset of Figure 4a, the adsorption of PEO onto PS NSs turns out to have two important consequences.[24] First, the measured Zeta potential on 1 μm PS NSs, which equals −50 mV in the absence of PEO, exhibits nearly logarithmic decay with PEO concentration in the range from 0.5 to 55 ppm as shown in Figure 4a. This suggests an effective screening of the coulomb repulsive force that subsequently reduces the separation d between NSs. Secondly, when $d \leq 2R_g$, it triggers the polymer bridging effect that provides further bonding between NSs. By analyzing the trajectories of 15 selected NSs each with 200 consecutive frames taken every 65 ms,

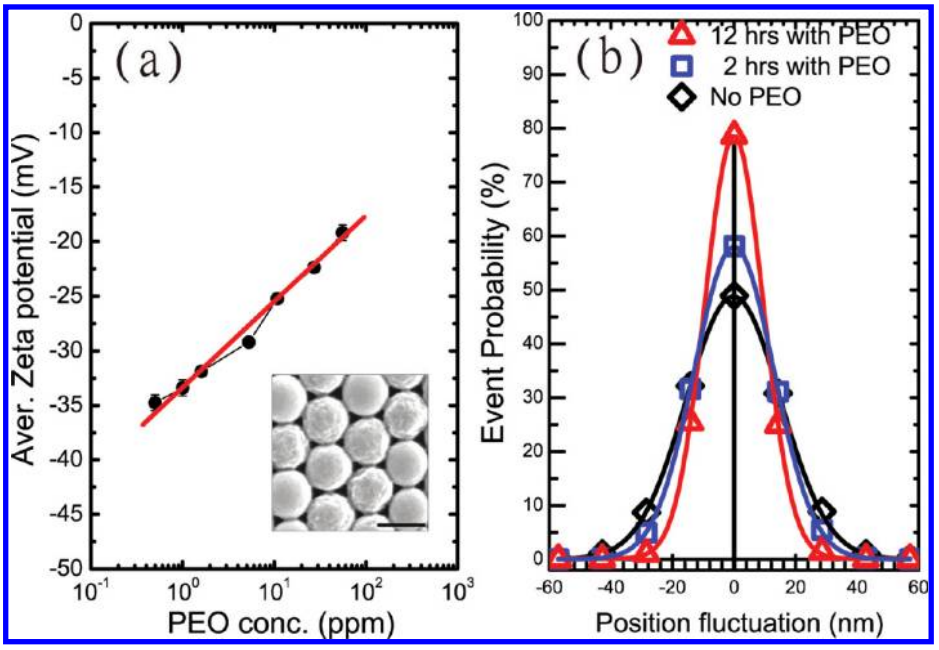

Figure 4. (a) Averaged Zeta potential on 1μm PS NSs as a function of PEO concentration in log scale. The red line is a linear fit to the data points. High-magnification SEM image shown in the inset reveals PEO residues on the NSs. The scale bar is 500 nm. (b) Histogram of position fluctuation obtained from a microscope equipped with a high-speed camera.

the obtained histogram of the position fluctuation (Figure 4b) with bin size of 14 nm shows a gradual evolution to a higher and narrower peak in PEO-bridged monolayer of NSs, indicating a strong suppression of Brownian motion due to PEO-bridging effect. To further confirm this scenario, we performed a control experiment by intentionally introducing 3 ppm NaPSS, which is a negatively charged polymer, in the DI water before adding equal amount of PEOs. No further reduction in d was ever observed after an extended period of time ($\geq$24 h). The formation of PEO/NaPSS complex[24] significantly hinders the PEOs adsorption onto the PS NSs, which is detrimental according to our scenario. We noticed that similar bridging effect has also been reported in several systems, such as DNA-linked nanoparticles,[25−27] dodecanethiol-ligated gold NSs[28] and covalently bonded copolymer NSs,[14] where special surface modification on NSs is required. In contrast, the polymer-bridging effect we uncovered derives from a different mechanism that has less constraint on the surface condition of NSs. However, we do note that the fabrication time for a monolayer of PEO/PS NSs hybrid using our method is greatly restricted by the slow process of the PEO adsorption onto PS NSs, which may take up to 12 h as demonstrated in Figure 4b.

CONCLUSIONS

In summary, we have demonstrated a novel approach to prepare a hybrid material comprising a polymer-bridged monolayer of close-packed NSs at water−air interface with various NSs diameters ranging from 100 nm to 1 μm. Its working principle involves the effective screening of coulomb repulsive forces between NSs due to the adsorption of PEOs onto NSs followed by the polymer crosslink between NSs. We argue that our method can extend to NSs with smaller diameters and also with different composition as long as the adsorption of proper water-soluble polymers onto NSs can be achieved. Because of the special bonding between NSs as evident from the suppression in Brownian motion, we remark that the resulting close-packed monolayer of PEO/NSs hybrid can be transferred onto a substrate of any kind, including a curved surface, without serious damage to its original packing structure. Our finding can be of particular importance when surface treatment and planar substrate for NSL are not possible.

AUTHOR INFORMATION

Corresponding Author

*E-mail: wlee@phys.sinica.edu.tw (W.L.L.); wtjuan@phys.sinica.edu.tw (W.T.J.).

ACKNOWLEDGMENT

The authors acknowledge the funding support from National Science Council in Taiwan and research program on nanoscience and nanotechnology at Academia Sinica, Taipei.

REFERENCES

(1) Hulteen, J. C.; Van Duyne, R. P. *J. Vac. Sci. Technol., A* **1995**, *13*, 1553–1558.
(2) Asakura, S.; Oosawa, F. *J. Polym. Sci.* **1958**, *33*, 183–192.
(3) Lin, K.; Crocker, J. C.; Prasad, V.; Schofield, A.; Weitz, D. A.; Lubensky, T. C.; Yodh, A. G. *Phys. Rev. Lett.* **2000**, *85*, 1770–1773.
(4) Kuo, C. W.; Shiu, J. Y.; Cho, Y. H.; Chen, P. *Adv. Mater.* **2003**, *15*, 1065–1068.
(5) Dimitrov, A. S.; Nagayama, K. *Langmuir* **1996**, *12*, 1303–1311.
(6) Weekes, S. M.; Ogrin, F. Y.; Murray, W. A.; Keatley, P. S. *Langmuir* **2007**, *23*, 1057–1060.
(7) Pan, F.; Zhang, J.; Cai, C.; Wang, T. *Langmuir* **2006**, *22*, 7101–7104.
(8) Rybczynski, J.; Ebels, U.; Giersig, M. *Colloids Surf., A* **2003**, *219*, 1–6.
(9) Kosiorek, A.; Kandulski, W.; Chudzinski, P.; Kempa, K.; Giersig, M. *Nano Lett.* **2004**, *4*, 1359–1363.

(10) Kosiorek, A.; Kandulski, W.; Glaczynska, H.; Giersig, M. *Small* **2005**, *1*, 439–444.
(11) Somobrata, A.; Jonathan, P. H.; Katsuhiko, A. *Adv. Mater.* **2009**, *21*, 2959–2981.
(12) Marquestaut, N.; Martin, A.; Talaga, D.; Servant, L.; Ravaine, S.; Reculusa, S.; Bassani, D. M.; Gillies, E.; Lagugne-Labarthet, F. O. *Langmuir* **2008**, *24*, 11313–11321.
(13) Kempa, K.; Kimball, B.; Rybczynski, J.; Huang, Z. P.; Wu, P. F.; Steeves, D.; Sennett, M.; Giersig, M.; Rao, D. V. G. L. N.; Carnahan, D. L.; Wang, D. Z.; Lao, J. Y.; Li, W. Z.; Ren, Z. F. *Nano Lett.* **2003**, *3*, 13–18.
(14) Hu, Z.; Lu, X.; Gao, J. *Adv. Mater.* **2001**, *22*, 1708–1712.
(15) Ashcroft, N. W.; Mermin, N. D. *Solid State Physics*; Harcourt: New York, 1976, 101.
(16) Silvan, M. M.; HernAndez, M. A.; Costa, V. T.; Palma, R. J. M.; Duart, J. M. M. *Europhys. Lett.* **2006**, *76*, 690–695.
(17) Ho, C. C.; Hsieh, T. W.; Kung, H. H.; Juan, W. T.; Lin, K. H.; Lee, W. L. *Appl. Phys. Lett.* **2010**, *96*, 122504.
(18) Kralchevsky, P. A.; Nagayama, K. *Langmuir* **1994**, *10*, 23–36.
(19) Stamou, D.; Duschl, C.; Johannsmann, D. *Phys. Rev. E* **2000**, *62*, 5263–5272.
(20) Nikolaides, M. G.; Bausch, A. R.; Hsu, M. F.; Dinsmore, A. D.; Brenner, M. P.; Gay, C.; Weitz, D. A. *Nature* **2002**, *420*, 299–301.
(21) Megens, M.; Aizenberg, J. *Nature* **2003**, *424*, 1014.
(22) Pieranski, P. *Phys. Rev. Lett.* **1980**, *45*, 569–572.
(23) Chen, W.; Tan, S.; Ng, T. K.; Ford, W. T.; Tong, P. *Phys. Rev. Lett.* **2005**, *95*, 218301.
(24) Qiu, D.; Cosgrove, T.; Revell, P.; Howell, I. *Macromolecules* **2009**, *42*, 547–552.
(25) Mirkin, C. A.; Letsinger, R. L.; Mucic, R. C.; Storhoff, J. J. *Nature* **1996**, *382*, 607–609.
(26) Alivisatos, A. P.; Johnsson, K. P.; Peng, X.; Wilson, T. E.; Loweth, C. J.; Bruchez, M. P.; Schultz, P. G. *Nature* **1996**, *382*, 609–611.
(27) Cheng, W. L.; Champolongo, M. J.; Cha, J. J.; Tan, S. J.; Umbach, C. C.; Muller, D. A.; Luo, D. *Nat. Mater.* **2009**, *8*, 519–525.
(28) Mueggenburg, K. E.; Lin, X. M.; Goldsmith, R. H.; Jaeger, H. M. *Nat. Mater.* **2007**, *6*, 656–660.